

EFFECT OF POWDER SIZE ON THE MICROSTRUCTURE AND MAGNETIC PROPERTIES OF Nd-Fe-B MAGNET ALLOY

Rare earth Nd-Fe-B, a widely used magnet composition, was synthesized in a shape of powders using gas atomization, a rapid solidification based process. The microstructure and properties were investigated in accordance with solidification rate and densification. Detailed microstructural characterization was performed by using scanning electron microscope (SEM) and the structural properties were measured by using X-ray diffraction. Iron in the form of α -Fe phase was observed in powder of about 30 μm . It was expected that fraction of $\text{Nd}_2\text{Fe}_{14}\text{B}$ phase increased rapidly with decrease in powder size, on the other hand that of α -Fe phase was decreased. Nd-rich phase diffused from grain boundary to particle boundary after hot deformation due to capillary action. The coercivity of the alloy decreased with increase in powder size. After hot deformation, $\text{Nd}_2\text{Fe}_{14}\text{B}$ phase tend to align to c-axis.

Keywords: Nd-Fe-B, Gas atomization, Powder size, Crystal orientation, Hot deformation

1. Introduction

Rare earth Nd-Fe-B magnet have the highest magnetic properties among all commercially available permanent magnets and they are ideal candidates for sophisticated applications as severe operating environment. Nd-Fe-B magnets are widely used in industries such as IT, MRI, automobile and wind generators [1-5]. Especially, in such automobile application such as hybrid electric vehicles (HEV) and electric vehicles (EV) it is necessary for the magnets to operate at temperature up to 150°C. Therefore it is important that increasing of the coercivity in order to enhance operating temperature. The coercivity is an important factor among magnetic properties and it is defined by the following equation (1) [4].

$$iH_c = \alpha H_A - N_{eff} M_s \quad (1)$$

Where iH_c is coercive force strength, α is factor related to the microstructure, H_A is anisotropic magnetic field, N_{eff} is the effective demagnetization field and M_s is saturation magnetization.

Usually the Nd-Fe-B magnet is synthesized using a rapid solidification based process such as strip casting and melt spinning, in accordance with microstructural refinement. In order to fabricate the final permanent magnet using those rapidly solidified stuffs, complicated consequent processes required such as hydrogen decrepitation (HD), jet milling, aligning and sintering. In case of latter required such as pulverization, pre-compaction and finally hot deformation [1]. These methods are

complex and the pulverized powder can be easily oxidized due to its large surface area. In the quest of alternative but relatively simple process of powder production, the authors propose gas atomization. Gas atomization provides high cooling rates and uniform microstructures in produced powders [6].

However the size of powder obtained from gas atomization is relatively larger than traditional methods which makes the grain size of powder coarsen, it makes the microstructure multi domain and isotropic in nature. Due to this reason the atomized powder is only used in bonded isotropic magnets until now because obtained powder from gas atomization is that it has low coercivity [6].

In order to overcome these limitations of gas atomized powder; the authors manufactured powder with Ar gas atomization followed by plastic deformation.

2. Experimental

Powder which composed with $\text{Nd}_{15.22}\text{Fe}_{78.63}\text{B}_{6.15}$ were fabricated by gas atomization system. Nd, Fe and B (99.99% purity) pellets were inductively melted (Model: DTIH-0050MF, Dongyang induction melting furnace, Korea) in alumina (Al_2O_3) crucible using boron nitride (BN) orifice and stopper. After melting, liquid melts were atomized with argon (Ar) gas at 3 MPa (30 bar) pressure. After atomization, the powder was collected and meshed into ≤ 24 , 25~44 and 45~75 μm size ranges respec-

* KOREA INSTITUTE FOR RARE METALS, KOREA INSTITUTE OF INDUSTRIAL TECHNOLOGY, GETBEOL-RO 12, SONGDO-DONG, INCHEON, 21999, KOREA

** HANYANG UNIVERSITY, DEPARTMENT OF MATERIAL SCIENCE AND CHEMICAL ENGINEERING, ANSAN, KOREA

*** UNIVERSITY OF SCIENCE AND TECHNOLOGY, CRITICAL MATERIALS AND SEMI-CONDUCTOR PACKAGING ENGINEERING, DAEJEON 3413, REPUBLIC OF KOREA

Corresponding author: tskim@kitech.re.kr

tively. Samples were polished and microstructural analysis was performed with scanning electron microscopy (FE-SEM; JEOL, JSM-7100F, Japan), the grain size and α -Fe fraction were measured by image analysis software (Image J) with powder size respectively. The powder was pre-compacted at 873K with spark plasma sintering (SPS; Welltech Co., SPS-20, Korea). After pre-compacting, the pre-compacted billet was hot deformed again by SPS. Hot deformation temperature was 1023K, strain ratio and strain rate were 64% and 0.001S^{-1} respectively. Magnetic measurements were carried out using vibrating sample magnetometer (VSM; Versalab, Quantum Design, Inc. USA) at room temperature. For VSM measurements 0.50 g of each sample was used. The applied magnetic field used for VSM measurements was 3T. Structural analysis was performed with X-ray diffractometer (XRD; D8-Advance, Bruker Miller, USA) with Cu K α radiation at 40 kV–30 mA settings and 2θ from 25° to 50° .

3. Results and discussion

Microstructures of powders from 10 μm to 90 μm are shown in Fig. 1 (a)~(e) respectively. The microstructure of as-atomized

powder consist of Nd-rich (white), $\text{Nd}_2\text{Fe}_{14}\text{B}$ (gray) and α -Fe (dark) phases respectively (Fig 1 (e)). The Nd-rich phase becomes coarsen with forming dendrites. It is known that Nd-Fe-B magnet, the $\text{Nd}_2\text{Fe}_{14}\text{B}$ phase is formed with under solidification rate faster than 10^3 K/s [1]. It is expected that this $\text{Nd}_2\text{Fe}_{14}\text{B}$ phase can accelerate reduction of α -Fe phase.

To observe the α -Fe phase fraction and the grain size with powder size, the microstructure was analyzed by Image J and the results are illustrated in Fig. 2 (a) and (b). Both the α -Fe phase fraction and the grain size are increased with increase of powder size. As shown in Fig. 2 (a) the α -Fe phase was observed initially at 30 μm , fraction of α -Fe phase grew relatively faster to 0.49% (Y_1) until 40 μm (X_1) and then relatively slow growth until 70 μm (X_2). After 70 μm α -Fe phase grew rapidly to 3.73% (Y_3) at over 80 μm (X_3). As shown in Fig. 2 (b), the grain size was sub-micron at 10 μm of powder size and then increased to about 6 μm at 90 μm of powder size. It is expected that due to mass effect of larger droplets which have larger grain size because larger atomized droplets achieve relatively low undercooling than smaller droplets.

The coercivity of atomized powder with powder size is shown in Fig. 3 [7]. The coercivity decreased with increase

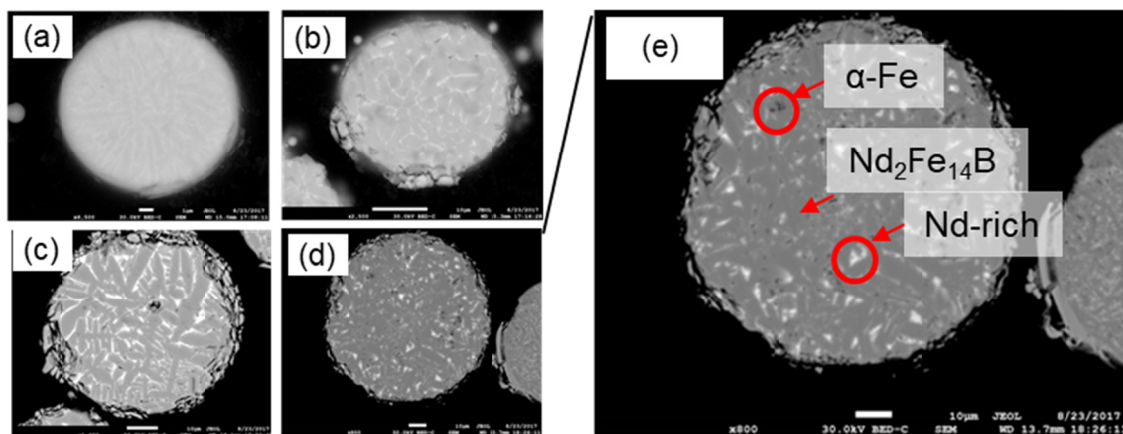


Fig. 1. Microstructure of atomized Nd-Fe-B powder with powder size (a) 10 μm , (b) 30 μm , (c) 60 μm , (d) 90 μm and (e) enlarged 90 μm respectively; Nd-rich (white), $\text{Nd}_2\text{Fe}_{14}\text{B}$ (gray) and α -Fe (dark)

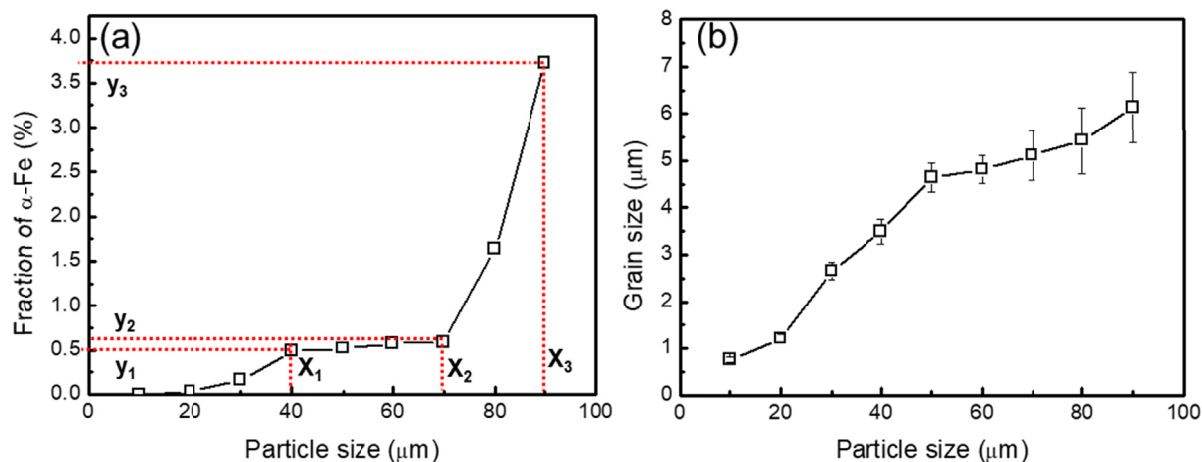


Fig. 2. Variation with powder size (a) fraction of α -Fe, (b) grain size

of powder size. Coercivity values were relatively lower than reference data (shown in red circles in Fig. 3) due to the fact that reference powder was fabricated by HDDR (hydrogen decrepitation desorption recombination) process, and their grain size was in range of dozens nanometer scale but in our case the smallest powder size which can be fabricated by using

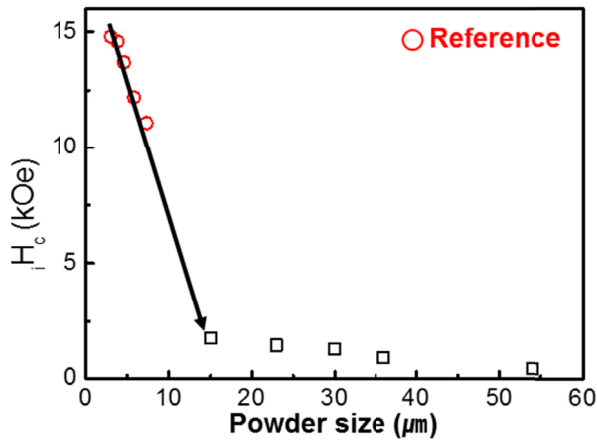


Fig. 3. Variation of the coercivity with powder size with reference data [8]

gas atomization was about 10 μm . Therefore it can be said that atomized powder has multi-domains, relatively larger grain size which makes coercivity relatively smaller. It can be expected that coercivity of atomized powder can be enhanced if powder size can be refined further.

To increase the magnetic property of multi-domain powder, plastic deformation was reported by Lee et al [8]. Since gas atomization process has limit to refine the powder size to submicron, the magnetic domain aligning through plastic deformation seems to be valuable by plastic deformation.

The microstructure with consolidated sample showing powder size under 25 μm , 25~45 μm and 45~75 μm after hot deformation are shown in Fig. 4. (a)~(c) respectively. The Nd-rich phase could not be found within grains in powders smaller than 45 μm but powders larger than 45 μm contain Nd-rich phase. It appears that the capillary action is enhanced in powders smaller than 45 μm but in powders greater than 45 μm Nd-rich phase remains in the grains probably due to capillary closure.

To observe the alignment to easy magnetization axis (c-axis) of the sample with powder size, the sample's diffraction data were measured and the result is shown in Fig. 5. As illustrated in Fig. 5, the atomized powders have similar tendency of alignment

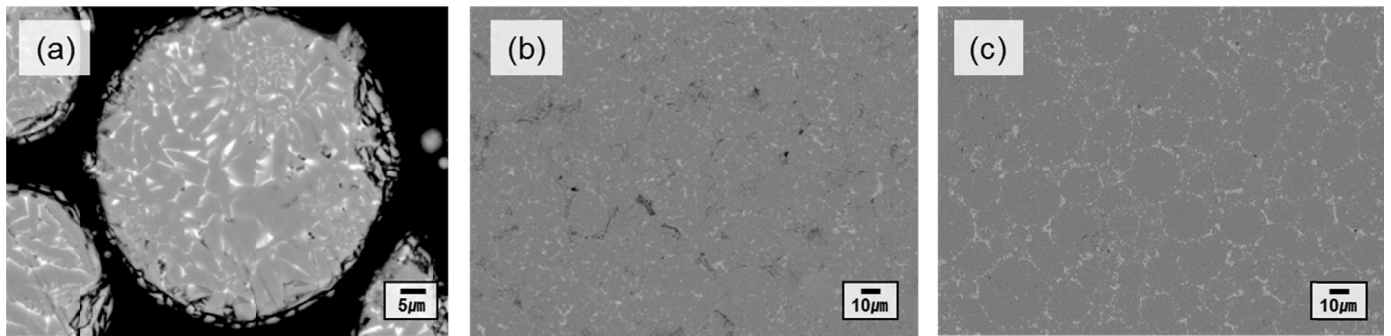


Fig. 4. Microstructure of (a) as powder, (b) pre-compacted billet and (c) hot deformed billet. Where Nd-rich (white), $\text{Nd}_2\text{Fe}_{14}\text{B}$ (gray) and pore (dark)

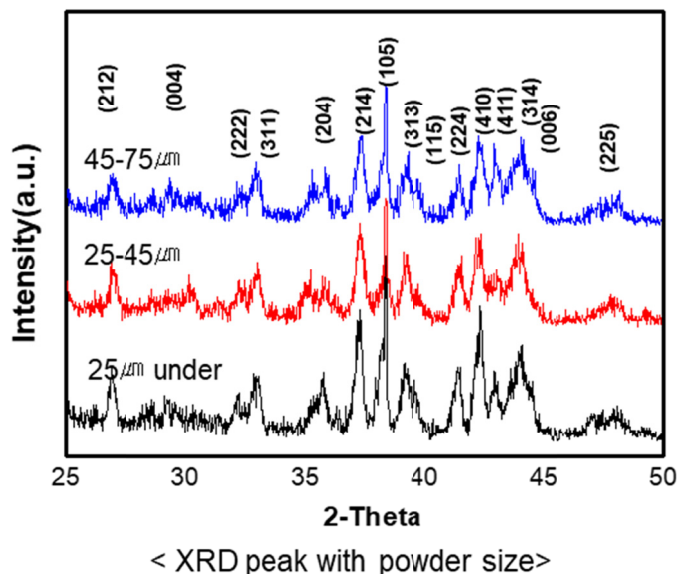


Fig. 5. Variation of alignment to c-axis with powder size after hot deformation process

of XRD peaks irrespective of powder size after hot deformation process.

Powders of 25~45 μm in size were hot deformed at 1023K and strain rate 0.001S^{-1} in order to confirm the process effect about alignment to c-axis. Fig. 6 (a)~(c) shows the SEM image of microstructure of the alloy with process. The Nd-rich phase of as atomized powder and pre-compacted billet formed inside grain boundary (Fig. 6 (b)) but after hot deformation process, it traversed to particle boundary. As the melting point of Nd-rich phase is about 873K [9], molten Nd-rich phase traversed to particle boundary due to capillary action (Fig. 6 (c)).

In Fig. 7, the orientation of highest plane of texture was changed with process from powder (410) to pre-compacted billet (214) and finally to hot deformed billet (105) planes respectively. It seems that $\text{Nd}_2\text{Fe}_{14}\text{B}$ phase was aligned to c-axis after plastic deformation. The texture of Nd-Fe-B can be changed during sintering process in order to match the surface energy [10]. But the alignment of atomized powder to c-axis even after hot-deformation process was not enough clear compared with melt

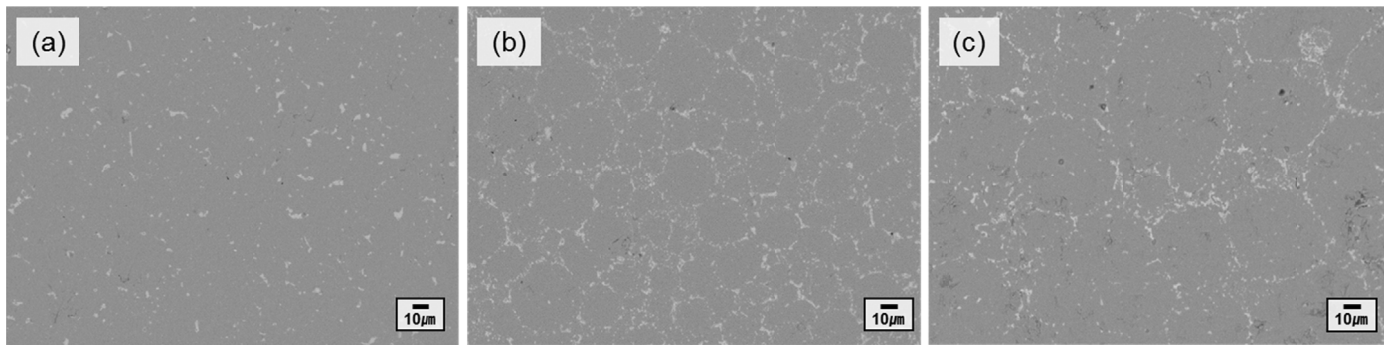


Fig. 6. Microstructure with powder size (a) $\sim 25 \mu\text{m}$, (b) $25\sim 45 \mu\text{m}$ and (c) $45\sim 75 \mu\text{m}$. Where Nd-rich (white), $\text{Nd}_2\text{Fe}_{14}\text{B}$ (gray) and $\alpha\text{-Fe}$ (dark)

spun powder [11]. In case of the melt spun powder, orientation is aligned to c-axis due to rotation of the nano sized grains by torque and perpendicular grain growth with c-axis [11, 12]. But the atomized powder cannot follow this mechanism because of large grain size. Even though the degree of aligning was not enough to satisfy for real application, further attempt on plastic deformation with alloy composition design will give a promising route of magnet fabrication.

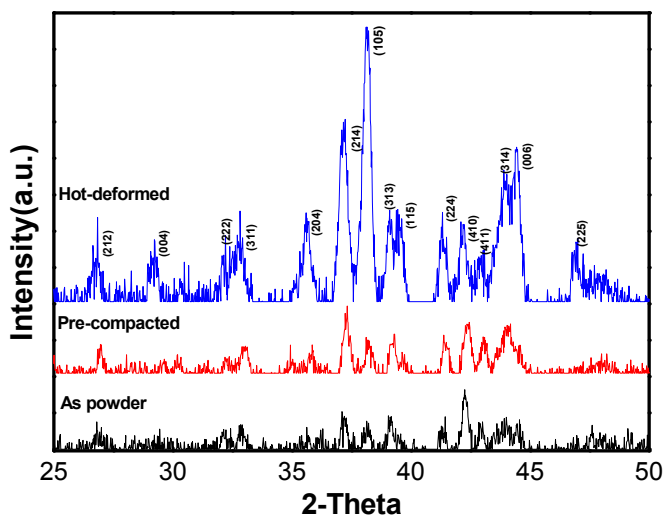


Fig. 7. Variation of alignment to c-axis with process

4. Conclusions

We have introduced a novel fabrication method about fabrication of Nd-Fe-B magnet using gas atomized powder. the powder has iron in $\alpha\text{-Fe}$ phase which exists in powders above $30 \mu\text{m}$ size and it grows with increase of powder size. Nd-rich

phase traversed to particle boundary from grain boundary with hot deformation process due to capillary action in powder size smaller than $45 \mu\text{m}$. The coercivity had low value compared to reference data but atomized powder seems to have enhanced coercivity after refining powder size. The alignment to easy magnetization axis (c-axis) is more uniform with process due to re-orientation during solid and liquid phase sintering. We believe atomized powder has the potential for fabrication of Nd-Fe-B magnet.

REFERENCES

- [1] S.G. Yoon, Transfer. Super Strong Permanent Magnets **1**, UUP, Ulsan (2002).
- [2] S.G. Yoon, Transfer. Rare Earth Permanent Magnet Materials and Their Applications **1**, UUP, Ulsan (1999).
- [3] C.J. Choe, Y.D. Han, Machinery and Materials **4**, 93 (1992).
- [4] J.G. Lee, J.H. Yu, Ceramist **17**, 50 (2014).
- [5] S. NamKung, S.K. Cho, J.B. Kim, Journal of the Korean Magnetism Society **22**, 221 (2012).
- [6] E. Vasilyeva, V. Vystavkina, Journal of Magnetic Materials **267**, 267 (2003).
- [7] K. Uestuener, M. Katter, W. Rodewald, IEEE Transactions on Magnetics **42**, 2897 (2006).
- [8] J.H. Lee, J.Y. Cho, S.W. Nam, S.F. Abbas, K.M. Lim, T.S. Kim, Science of Advanced Materials **9**, 1859 (2017).
- [9] Y. Luo, N. Zhang, C.D. Gragam, Jr. J. Appl. Phys. **61**, 3442 (1987).
- [10] G. Petzow, H.E. Exner, Advanced Technical Ceramics **67**, 611 (1976).
- [11] H.Y. Yasuda, M. Kumano, T. Nagase, R. Kato, H. Shimizu, Scr. Mater. **65**, 743 (2011).
- [12] W.A. Kaysser, G. Petzow, Powder Metallurgy **28**, 145 (1985).